Experimental and numerical investigations of a pendulum driven by a low-powered DC motor (NUM305-15)

Grzegorz Wasilewski, Grzegorz Kudra, Jan Awrejcewicz, Maciej Kaźmierczak, Mateusz Tyborowski, Marek Kaźmierczak

Abstract: The work is a continuation of numerical and experimental investigations of a system consisting of a single pendulum with the joint horizontally driven by the use of a crank-slider mechanism and DC motor. The power supplied to the DC motor is relatively small when compared with our earlier investigations, which results in clear return influence of the pendulum dynamics on the DC motor angular velocity and much more rich bifurcation dynamics of the whole system, including regions of chaotic behaviour. In the experiments, the motor is supplied by the use of different but constant in time voltages. A series of experiments allow for accurate estimation of the model parameters and, in the further step, for prediction of the real system behaviour, also for other functions representing input voltage, including the time-varying ones.

1. Introduction

There exist a lot of studies on non-linear dynamics of mechanical systems composed of pendulums in different configurations, including plane or spatial, single or multiple, and sometimes parametrically excited pendulums. Physicians are particularly interested in those kinds of the dynamical systems, since they are relatively simple but can exhibit almost all aspects and phenomena of non-linear dynamics. In some case an experiment is performed in order to confirm analytical or numerical investigations [1-3]. Sometime, in order to achieve a good agreement between the model's predictions and experimental data, one must take into account many details concerning physical modelling of the real process [3].

When considering behavior of the real dynamical systems one can encounter a problem of mutual interactions between the oscillatory system and the energy source of limited power, i.e. non-ideal energy source. Belato et al. [4] investigated numerically the electro-mechanical system composed of a pendulum excited by a crank-shaft-slider mechanism driven by a DC motor considered as a limited power source. A comprehensive numerical analysis of bifurcational dynamics of a similar mechanical system is presented in [5]. An extensive review on the non-ideal vibrating systems one can find in [6].

In the work [7], the authors investigated both numerically and experimentally an electro-mechanical system consisting of a pendulum suspended on the slider of a crank-slider mechanism driven by a DC motor. Since the power of the motor was relatively high, the angular velocity of the

shaft was almost constant. Mathematical modelling of the same system under simplifying assumption of a constant angular velocity of the crank, together with the improved algorithm of the parameters' estimation, is presented in [8].

In the present work, the same structure of the mathematical model as in [7] is used in the analysis of the similar real electro-mechanical system, but in the case of relatively low power supplied to the DC motor, resulting in more variable angular velocity of the crank.

2. Experimental rig

Figure 1 presents the experimental setup of mathematical model that will be described in next part of the paper. A voltage generator 1 supplies the low power DC motor 3. Output shaft of the motor is connected with steel shaft 5 by aluminium coupling 4. Shaft 5 is embedded in pair of ball bearings 6 that provides alignment of shafts. Ball bearings are mounted on 'L' bracket 7a with additional two brackets in 'C' 7b and 'L' 7c shape that support first one to be more stable. Two aluminium strips 7d act as rails to set 'L' bracket both with ball bearings and with DC motor to set them in right position.

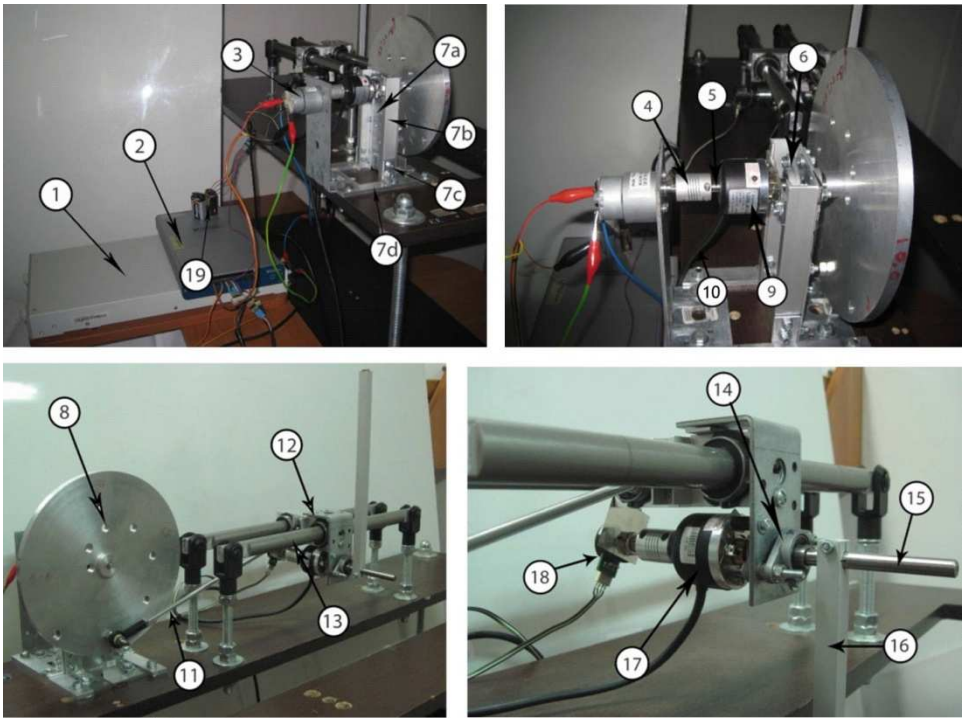

Figure 1. Experimental setup

There is also the possibility to change low power DC motor into other one with higher power. On the other end of shaft 5 there is mounted disk 8. Angular position of disk is measured by the use of

encoder 9 (type MHK, 360 steps) supplied by wire 10. Rotational motion of disk is transformed thanks to joint 11 (connecting bar) into linear motion of the slider 12 moving on two horizontal guides 13. To the slider there is mounted bracket with two ball bearings 14 (same type as 5) and shaft 15 inserted into them. On this part there is seated physical pendulum 16. In identical way like disk, angular position of pendulum is measured by two types of encoders. 17 is the same type like in case of measuring position of disk. Encoder 18 (type MAB-analog out, supplied by to batteries 19) is used to perform longer measurement, because encoder 17 (type MHK, 3600 steps) have a high resolution what really quickly fills up available space on PC hard disk. All data from encoders are collected by data acquisition 2.

3. Mathematical modelling

In this section there is presented the mathematical model of the experimental rig presented in section 2. It is based on the results published in the work [7]. Figure 2(a) exhibits a block diagram presenting the general structure of the system. It is composed of two main subsystems: i) DC motor (understood as a pure electrical object converting the electrical energy to the mechanical torque; ii) a two-degree-of –freedom mechanical system including all mechanical elements of the system. The input signal (being under control) is the voltage $u(t)$ supplied to the DC motor. The two coordinates $\theta(t)$ and $\varphi(t)$ determining the position of the mechanical system are assumed to be outputs.

For an armature controlled DC motor equipped with a gear transmission and assuming that the armature inductance is negligible, one gets the following equation

$$M = \frac{K_T}{R} i_g u - \frac{K_E K_T}{R} i_g^2 \frac{d\theta}{dt}, \tag{1}$$

where M is the torque on the output shaft of the gear transmission, u – input voltage, θ – angular position of the output shaft of the gear transmission, i_g – reduction ratio of the gear transmission, R – armature resistance, K_T – the proportionality constant between the torque generated on the output shaft of the DC motor and the armature current, K_E - the proportionality constant between the back electromotive force and the angular velocity of the DC motor.

A sketch of a physical model of the mechanical section of the system is depicted in figure 2(b). This plane two-degree-of-freedom mechanical systems is composed of four rigid bodies (1- disk, 2 – connecting bar, 3 – slider, 4 - pendulum) connected by the use of four rotational joints (O, A, B_1 and B_2). Masses of the links 2-4 are denoted as m_b, m_S and m, respectively. Moments of inertia of the bodies 1, 2 and 4, with respect to their mass centers (located in the points O, C_2 and C_4), are represented by the symbols I_O, I_b and I, respectively. The corresponding lengths of the mechanical system are denoted as follows: $a=OA$, $b=AB$, $b_1=AC_2$ and $r=BC_4$. The position of the system is determined by two angles: θ - angular position of the disk (equal to the angular position of the gear

transmission output shaft) and φ – angular position of the pendulum. The disk 1 represents all rotating elements of the DC motor, gear transmission and real disk of the experimental rig.

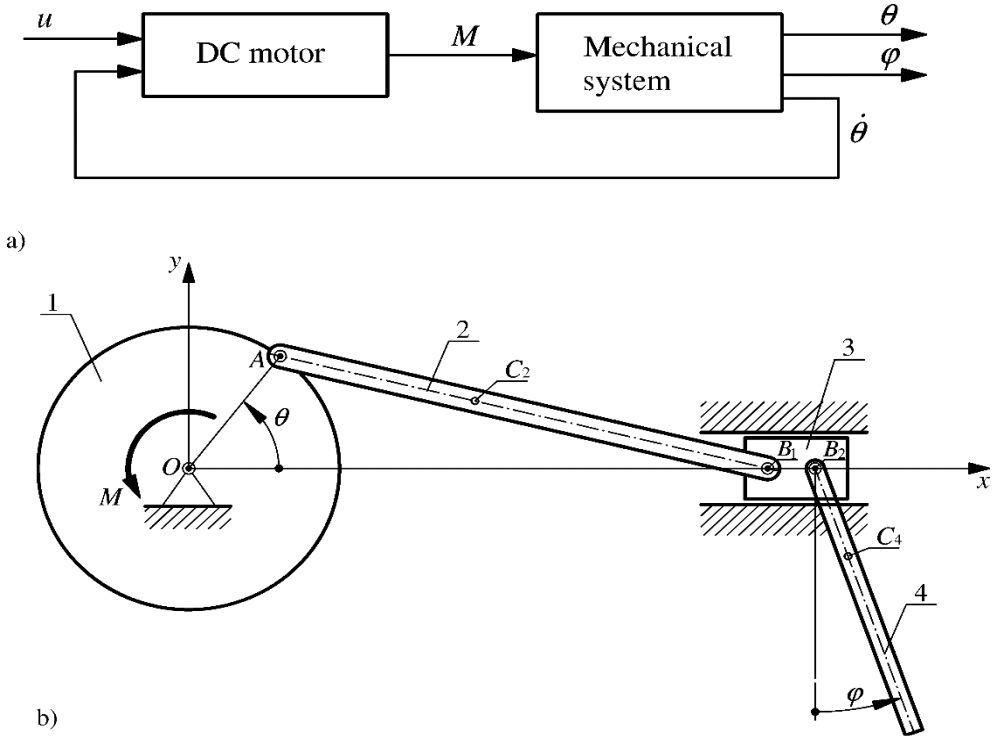

Figure 2. Physical model of the system

The governing equations of the investigated system read

$$\mathbf{M}(\mathbf{q})\ddot{\mathbf{q}} + \mathbf{N}(\mathbf{q})\dot{\mathbf{q}}^{\mathbf{2}} + \mathbf{w}(\mathbf{q}) = \mathbf{f}(t) - \mathbf{r}(\mathbf{q}, \dot{\mathbf{q}}), \tag{2}$$

where

$$\mathbf{q} = \begin{Bmatrix} \theta \\ \varphi \end{Bmatrix}, \quad \dot{\mathbf{q}} = \begin{Bmatrix} \dot{\theta} \\ \dot{\varphi} \end{Bmatrix}, \quad \ddot{\mathbf{q}} = \begin{Bmatrix} \ddot{\theta} \\ \ddot{\varphi} \end{Bmatrix}, \quad \dot{\mathbf{q}}^{\mathbf{2}} = \begin{Bmatrix} \dot{\theta}^2 \\ \dot{\varphi}^2 \end{Bmatrix},$$

$$\mathbf{M}(\mathbf{q}) = \begin{bmatrix} I_O + a^2(F^2(m+m_S) + F_1^2 m_b) + \dfrac{a^2}{b^2}\cos^2\theta((b-b_1)^2 m_b + G^2 I_b) & -amrF\cos\varphi \\ -amrF\cos\varphi & I + mr^2 \end{bmatrix},$$

$$\mathbf{N}(\mathbf{q}) =$$

$$= \begin{bmatrix} aFH\left(1+\dfrac{m_S}{m}\right) + aF_1H_1 - \dfrac{a^2}{2b^2}\sin 2\theta\left((b-b_1)^2 m_b + G^2 I_b\left(1 - \dfrac{a^2}{b^2}G^2\cos^2\theta\right)\right) & amrF\sin\varphi \\ -rH\cos\varphi & 0 \end{bmatrix},$$

$$\mathbf{w}(\mathbf{q}) = \begin{Bmatrix} \frac{a}{b}(b-b_1)m_b g\cos\theta \\ mgr\sin\varphi \end{Bmatrix}, \quad \mathbf{f}(t) = \begin{Bmatrix} M(t) \\ 0 \end{Bmatrix}, \quad \mathbf{r}(\mathbf{q}, \dot{\mathbf{q}}) = \begin{Bmatrix} M_{R\theta}(\theta, \dot{\theta}) \\ M_{R\varphi}(\dot{\varphi}) \end{Bmatrix}, \tag{3}$$

and where one has used the following notation

$$G = \frac{1}{\sqrt{1-\frac{a^2}{b^2}\sin^2\theta}}, \quad F = \left(1+\frac{a}{b}G\cos\theta\right)\sin\theta, \quad F_1 = \left(1+\frac{ab_1}{b^2}G\cos\theta\right)\sin\theta,$$

$$H = am\left(\cos\theta + \frac{a}{b}G\cos 2\theta + \frac{1}{4}\frac{a^3}{b^3}G^3\sin^2 2\theta\right),$$

$$H_1 = am_b\left(\cos\theta + \frac{ab_1}{b^2}G\cos 2\theta + \frac{1}{4}\frac{a^3b_1}{b^4}G^3\sin^2 2\theta\right). \tag{4}$$

The vector $\mathbf{r}(\mathbf{q}, \dot{\mathbf{q}})$ contains all resistance forces and their components:

$$M_{R\theta}(\theta, \dot{\theta}) = c_O\dot{\theta} + \frac{2}{\pi}M_O\arctan(\varepsilon\dot{\theta}) + a^2F^2c_S\dot{\theta} - \frac{2}{\pi}aFT_S\arctan(-\varepsilon aF\dot{\theta}),$$

$$M_{R\varphi}(\dot{\varphi}) = c_B\dot{\varphi} + \frac{2}{\pi}M_B\arctan(\varepsilon\dot{\varphi}), \tag{5}$$

The terms $c_O\dot{\theta}$ and $\frac{2}{\pi}M_O\arctan(\varepsilon\dot{\theta})$ represent the viscous damping and dry friction components of the resistance in the joint *O*, where c_O is viscous damping coefficient, M_O - magnitude of dry friction torque, while ε is large numerical parameter used in the dry friction model regularization. One assumes that M_O is a constant parameter, independent from the loading of the joint *O*. The expressions $a^2F^2c_S\dot{\theta}$ and $-\frac{2}{\pi}aFT_S\arctan(-\varepsilon aF\dot{\theta})$ represents the viscous damping and dry friction components of resistance between the slider and guide, reduced to the coordinate θ, where c_S and T_S are the corresponding constant parameters. Similarly, the terms $c_B\dot{\varphi}$ and $\frac{2}{\pi}M_B\arctan(\varepsilon\dot{\varphi})$ are viscous damping and dry friction components in the joint B_2. Resistances in the joints *A* and B_1 are not taken into account.

Finally one gathers the right-hand side of Eq. (6) into one vector:

$$\mathbf{f}_r(t, \mathbf{q}, \dot{\mathbf{q}}) = \mathbf{f}(t) - (\mathbf{q}, \dot{\mathbf{q}}) =$$

$$= \begin{Bmatrix} K_M u(t) - C_O\dot{\theta} - \frac{2}{\pi}M_O\arctan(\varepsilon\dot{\theta}) - a^2F^2c_S\dot{\theta} + \frac{2}{\pi}aFT_S\arctan(-\varepsilon aF\dot{\theta}) \\ -c_B\dot{\varphi} - \frac{2}{\pi}M_B\arctan(\varepsilon\dot{\varphi}) \end{Bmatrix}, \tag{6}$$

where

$$K_M = \frac{K_T}{R}i_g, \quad C_O = \frac{K_EK_T}{R}i_g^2 + c_O.$$

Let us note, that the mechanical viscous damping in the joint *O* and the back electromotive force (multiplied by some other constants) have mathematically the same influence on the final torque on the output shaft of the gear transmission. They are mathematically indistinguishable and unidentifiable in the developed model. Their aggregate action is defined by the coefficient C_O.

4. Parameter estimation

In the process of identification, one has used four experimental solutions, with the input signal $u(t)$ in a form of step function with zero initial value, and constant final value u0, equal to -7, -7.5, -8.0 and -8.5 V, respectively. The initial conditions are the same for all experiments: $\theta(0) = -\frac{\pi}{2}\text{rad},\ \varphi(0) = 0\ \text{rad},\ \dot{\theta}(0) = 0\ \text{rad/s}$ and $\dot{\varphi}(0) = 0\ \text{rad/s}$. The solutions tend to periodic attractors, which allows to avoid problems of identification related to high sensitivity to initial conditions. The angles $\varphi(t)$ and $\theta(t)$ were recorded on the time interval [0, 100] s.

Because of non-ideal behavior of resistances in the system (small random fluctuations of friction), the angular velocity of the disk undergoes some random changes, which cannot be described by the use of deterministic equations. These changes are not big, but after some time they can lead to significant time shift in the angular position of the disk. It may cause problems in fitting of the simulated signals to those obtained experimentally, if we express them in the time domain. This is the reason of the idea to compare the corresponding signals expressed as functions of angular position of the disk θ.

Since we plan to use in the estimation process two different signals (angular position of the pendulum and angular velocity of the disk), we construct the objective function F_o in the form of weighted sum of two different parts:

$$F_O(\boldsymbol{\mu}) = w_\varphi F_{O\varphi}(\boldsymbol{\mu}) + w_\omega F_{O\omega}(\boldsymbol{\mu}), \tag{7}$$

where $\boldsymbol{\mu}$ is vector of the estimated parameters, w_φ and w_ω are the corresponding weights, and where

$$F_{O\varphi}(\boldsymbol{\mu}) = \frac{1}{\sum_{i=1}^{N}\theta_{fi}}\sum_{i=1}^{N}\int_{\theta_0}^{\theta_{fi}}\left(\varphi_{si}(\theta,\boldsymbol{\mu}) - \varphi_{ei}(\theta,\boldsymbol{\mu})\right)^2 d\theta,$$

$$F_{O\omega}(\boldsymbol{\mu}) = \frac{1}{\sum_{i=1}^{N}\theta_{fi}}\sum_{i=1}^{N}\int_{\theta_0}^{\theta_{fi}}\left(\omega_{fsi}(\theta,\boldsymbol{\mu}) - \omega_{fei}(\theta,\boldsymbol{\mu})\right)^2 d\theta. \tag{8}$$

In the expressions (8) N denotes number of the compared pairs of solutions, θ_0 is common initial angle θ, θ_{fi} (i=1, 2, …, N) are final angular positions of the disk, φ_{si} and φ_{ei} are angular positions of the pendulum obtained by the use of i-th numerical simulation and experiment, correspondingly. Since we measure the angular position of the disk, we differentiate this signal with respect to time in order to obtain the corresponding angular velocity. We do it numerically, by passing the signal $\theta_{ei}(t)$ (obtained by the linear interpolation of the experimental data) through the filter of the transfer function $G_f(s) = \frac{s}{(T_f s+1)^2}$. As an output we obtain the signal $\omega_{fei}(t)$, which appears in the expressions (8), but as a function of the angle θ. In order to have the proper simulation signal, which

could be compared with the signal ω_{fei}, we also pass through the filter $G_f(s)$ the numerical signal $\theta_{si}(t)$, obtaining $\omega_{fsi}(t)$.

In the estimation process one obtained the following values of the model parameters: $K_M = 3.024 \cdot 10^{-2}$N m/V, $C_O = 2.915 \cdot 10^{-2}$N m s, $M_O = 3.032 \cdot 10^{-2}$N m, $I_O = 5.724 \cdot 10^{-3}$kg m^2, $I_b = 5.318 \cdot 10^{-4}$kg m^2, $b_1 = 1.026 \cdot 10^{-1}$m, $c_S = 3.597 \cdot 10^{-1}$N s, $T_s = 6.172 \cdot 10^{-1}$N, $I = 1.258 \cdot 10^{-3}$kg m^2, $r = 4.689 \cdot 10^{-2}$m, $c_B = 6.830 \cdot 10^{-5}$N m s, $M_B = 2.977 \cdot 10^{-3}$N m. Figure 3 exhibits comparison of four numerical solutions $\varphi(\theta)$ to the model with the corresponding experimental data used during the identification process (only the final parts of the solutions are presented). In figure 4 there are presented comparison of the corresponding solutions $\omega_f(\theta)$.

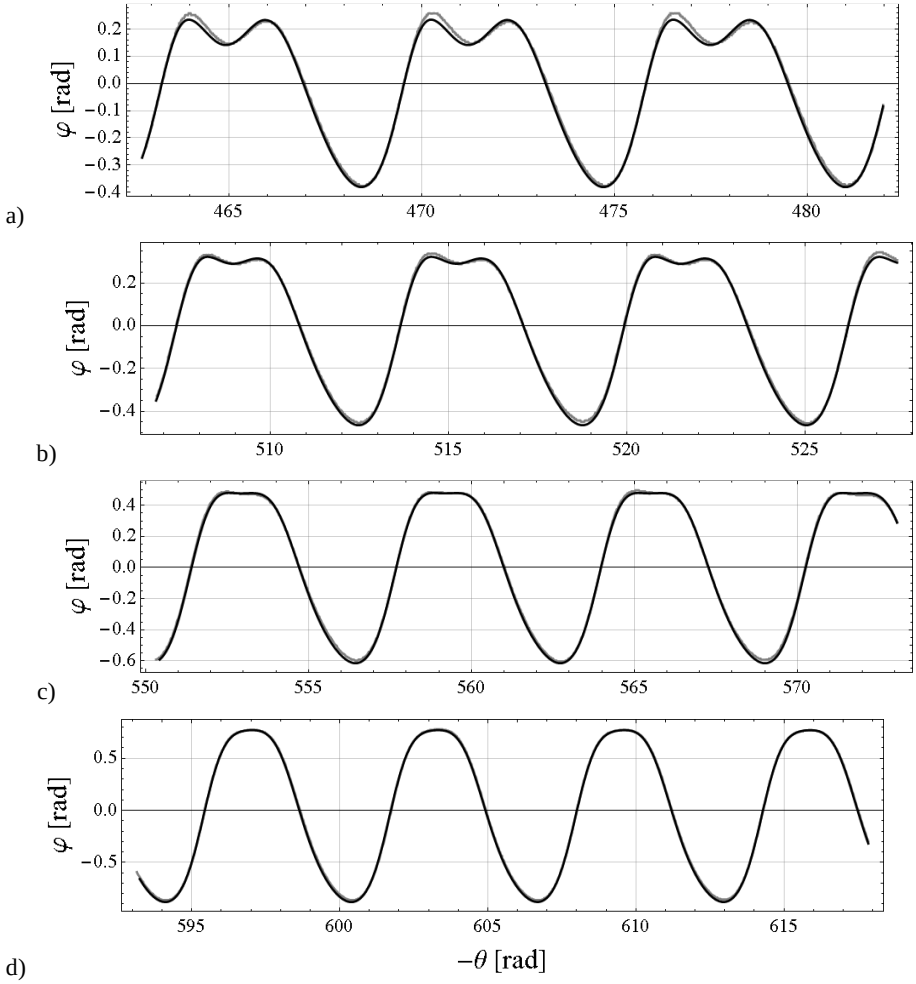

Figure 3. Four numerical solutions $\varphi(\theta)$ (black line) compared with the corresponding experimental data (gray line) (u_0=-7.0, -7.5, -8.0 and -8.5 V, for subfigures a, b, c and d, respectively).

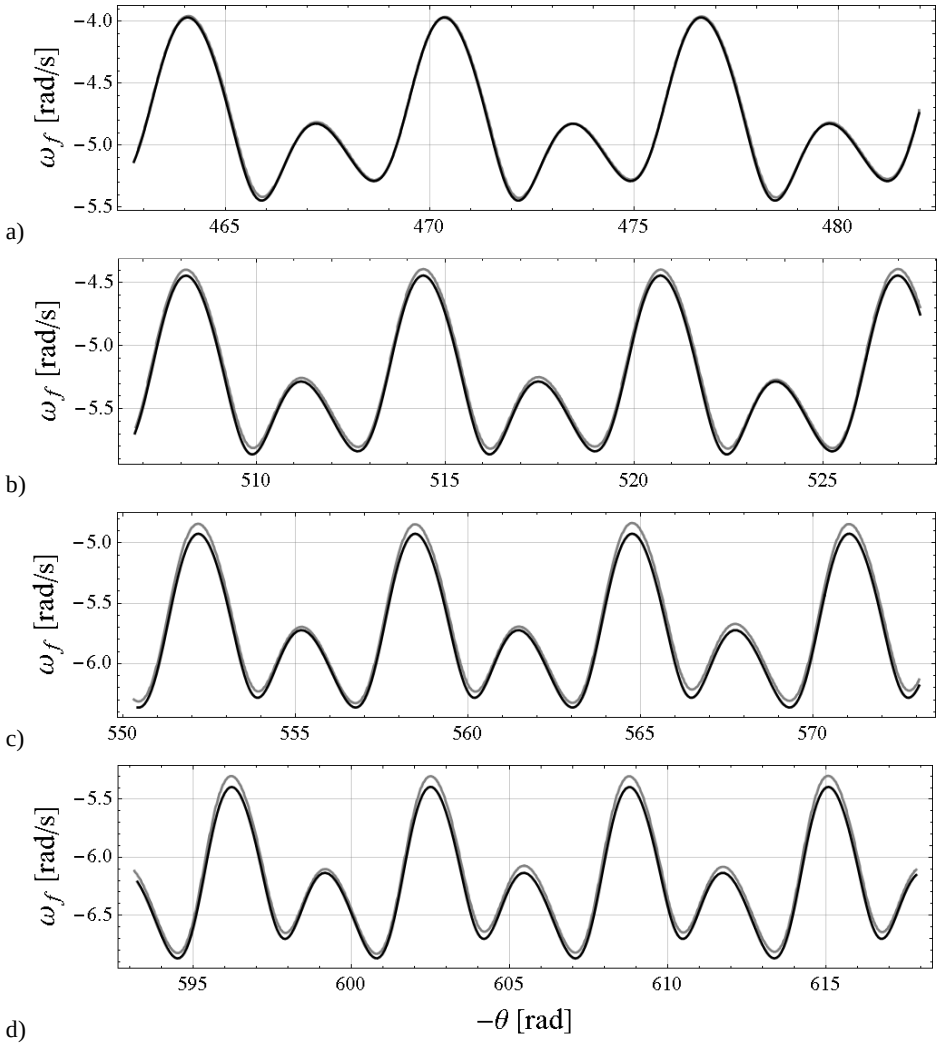

Figure 4. Four numerical solutions $\omega_f(\theta)$ (black line) compared with the corresponding experimental data (gray line) (u_0=-7.0, -7.5, -8.0 and -8.5 V, for subfigures a, b, c and d, respectively).

Using the functions (8), one assumes that initial conditions and input signals $u(t)$ are known and they are the same for both the experiment and simulation. Moreover, some parameters' values are easy to obtain by the direct measurements of masses and lengths. They are assumed to be constant during the identification process: $m_b = 0.035$ kg, $m_S = 0.777$ kg, $m = 0.226$ kg, $a = 0.080$ m, $b = 0.300$ m. Other parameters assumed to be constant are: $\varepsilon = 10^3$, $g = 9.81\ \mathrm{m \cdot s^{-2}}$. The remaining parameters (as the elements of the vector $\boldsymbol{\mu}$) will be obtained by minimization of the objective function F_o, using the Nelder-Mead method [9, 10], also known as downhill simplex

method. This is commonly used optimization algorithm, implemented in Matlab and Scilab functions *fminsearch*. One also assumes the following values of the weights and the time constant of the filter: $w_\varphi = 1\text{rad}^{-2}$, $w_\omega = 1\ \text{s}^2\text{rad}^{-2}$, $T_f = 0.1$ s.

5. Bifurcation dynamics

Other experimental investigations of the systems showed that it can also exhibit irregular behavior. For example the constant input voltage of 9 V leads to irregular dynamics, with full rotations of the pendulum, presented in figure 5. This solutions did not be used in the identification process because of potential problems related to high sensitivity to initial conditions. However they are confirmed qualitatively very well by the developed mathematical model and its numerical simulations, as shown in figure 5.

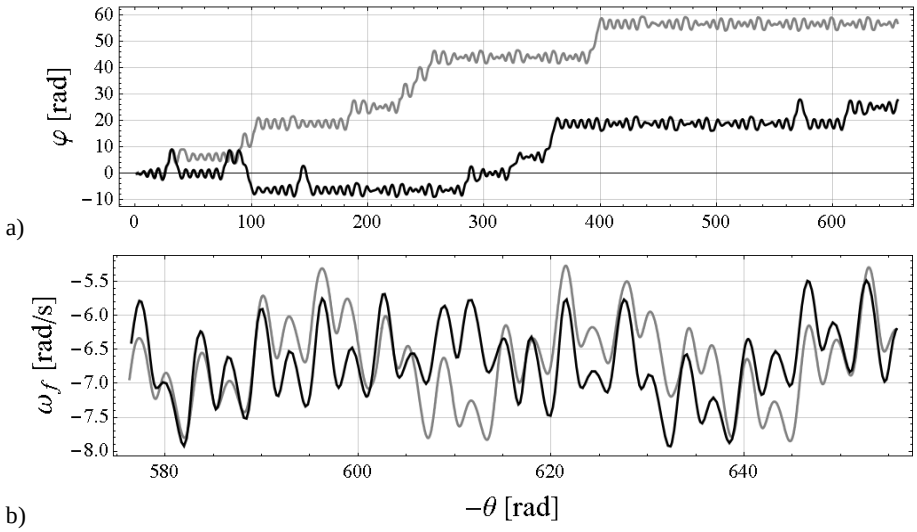

Figure 5. The chaotic numerical solutions (black lines) $\varphi(\theta)$ (a) and $\omega_f(\theta)$ (b) compared with the corresponding experimental data (gray lines) for u_0=-9 V.

In figure 6 there is presented Poincaré section of the attractor (sampling of the system state at the instances, when the angular position $\theta(t)$ of the disk crosses the zero position) exhibited by mathematical model for u_0=-9 V. It indicates the chaotic character of the solution. Figure 7 exhibits the corresponding bifurcation diagram of the mathematical model (for quasi-statically changing the bifurcation parameter u_0 from -7 V to -10 V), confirming the chaotic window around the value u_0=-9 V and many other zones of interesting bifurcational dynamics.

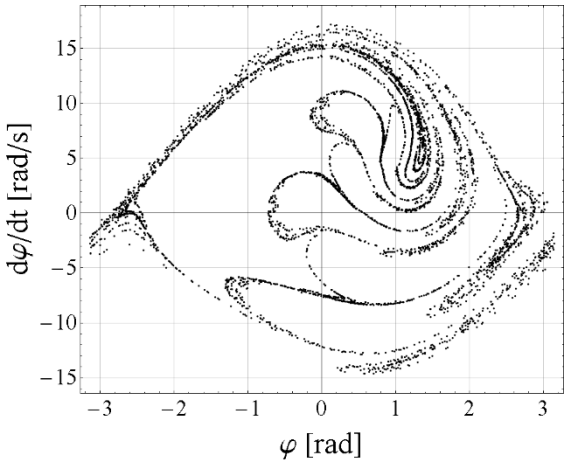

Figure 6. Poincaré section of the chaotic attractor obtained numerically for u_0=-9.0 V.

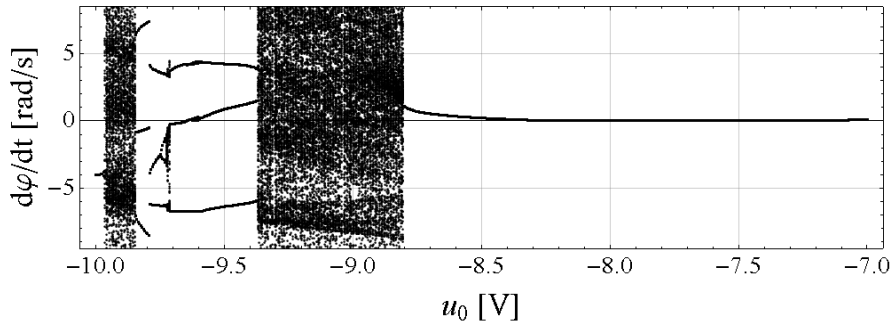

Figure 7. Bifurcation diagram with constant in time input voltage u_0 as a control parameter.

6. Concluding remarks

The paper presents results of the first stage of the larger project, which aim will be numerical and experimental investigation of different configurations of an electro-pendulum system. Here we have developed a simulation model of existing real object consisting of a physical pendulum hung on a horizontal slider, which is driven by a DC motor and a mechanism converting the rotational motion to the rectilinear one. Because of the goal of the project stage, the developed mathematical model is complicated and includes detailed modelling of friction and damping in the system.

Despite a relatively poor a priori knowledge about the system (especially knowledge about the DC motor and the gear transmission), using four time series with different constant values of the input voltage and a few direct measurements of physical quantities (like masses and lengths), we developed the mathematical model, which maps the behavior of the real object very well.

It has been shown in the work, that the built simulation model can be used for both explanation and prediction of nonlinear dynamics phenomena exhibited by the real electro-pendulum. On the other hand, the paper presents only preliminary results of the work being in progress. It is planned, among others, to investigate in more detail the bifurcational dynamics of the system with a constant input voltage, but also in the case of different types of periodic input.

Acknowledgments

This work has been supported by the Polish National Science Centre, MAESTRO 2, No. 2012/04/A/ST8/00738.

References

[1] Blackburn, J.A., Zhou-Jing, Y., Vik, S., Smith, H.J.T., and Nerenberg, M.A.H. Experimental study of chaos in a driven pendulum. *Physica D* 26, 1-3 (1987), 385-395.

[2] Zhu, Q., and Ishitobi, M. Experimental study of chaos in a driven triple pendulum. *Journal of Sound and Vibration*, 227, 1 (1999), 230-238.

[3] Awrejcewicz, J., Supeł, B., Kudra, G., Wasilewski, G., and Olejnik, P. Numerical and experimental study of regular and chaotic motion of triple physical pendulum. *International Journal of Bifurcation and Chaos* 18, 10 (2008), 2883-2915.

[4] Belato, D., Weber, H.I., Balthazar, J.M., and Mook, D.T. Chaotic vibrations of a nonideal electro-mechanical system. *International Journal of Solids and Structures*, 38 (2001), 1699-1706.

[5] Avanço, R.H., Navarro, H.A., Brasil, R.M.L.R.F., and Balthazar, J.M. Nonlinear Dynamics of a Pendulum Excited by a Crank-Shaft-Slider Mechanism, *ASME 2014 International Mechanical Engineering Congress and Exposition, Volume 4B: Dynamics, Vibration, and Control*, Montreal, Quebec, Canada, 2014.

[6] Cveticanin, L. Dynamics of the non-ideal mechanical systems: A review. *Journal of the Serbian Society for Computational Mechanics* 4, 2 (2010), 75–86.

[7] Kaźmierczak, M., Kudra, G., Awrejcewicz, J., and Wasilewski, G. Numerical and experimental investigation of bifurcational dynamics of an electromechanical system consisting of a physical pendulum and DC motor, in: Awrejcewicz J, Kaźmierczak M, Olejnik P and Mrozowski J (eds.) *Dynamical Systems – Applications.* TU of Lodz Press, Lodz, 2013, 49-58.

[8] Kaźmierczak, M., Kudra, G., Awrejcewicz, J., and Wasilewski, G. Mathematical modelling, numerical simulations and experimental verification of bifurcation dynamics of a pendulum driven by a dc motor. *European Journal of Physics* 36, 5 (2015), 13 pp.

[9] Gershenfeld, N. *The Nature of Mathematical Modelling*. Cambridge University Press, 2011.

[10] Nelder, J.A., and Mead, R. A simplex method for function minimization. *Computer Journal* 7, 4 (1965), 308-313

Grzegorz Wasilewski, Ph.D.: Lodz University of Technology, Department of Automation, Biomechanics and Mechatronics, Stefanowski St. 1/15, 90-924 Lodz, Poland (*grzegorz.wasilewski@p.lodz.pl*).

Grzegorz Kudra, Ph.D., D.Sc.: Lodz University of Technology, Department of Automation, Biomechanics and Mechatronics, Stefanowski St. 1/15, 90-924 Lodz, Poland (*grzegorz.kudra@p.lodz.pl*). The author gave a presentation of this paper during one of the conference sessions.

Jan Awrejcewicz, Professor: Lodz University of Technology, Department of Automation, Biomechanics and Mechatronics, Stefanowski St. 1/15, 90-924 Lodz, Poland (*jan.awrejcewicz@p.lodz.pl*).

Maciej Kaźmierczak (B.Sc. student): Lodz University of Technology, Department of Automation, Biomechanics and Mechatronics, Stefanowski St. 1/15, 90-924 Lodz, Poland (*182720@edu.p.lodz.pl*).

Mateusz Tyborowski (B.Sc. student): Lodz University of Technology, Department of Automation, Biomechanics and Mechatronics, Stefanowski St. 1/15, 90-924 Lodz, Poland (*182777@edu.p.lodz.pl*).

Marek Kaźmierczak, M.Sc.: Lodz University of Technology, Department of Automation, Biomechanics and Mechatronics, Stefanowski St. 1/15, 90-924 Lodz, Poland (*marek.kazmierczak.1@p.lodz.pl*).